

Elastic Scattering of Nitrogen by Carbon

M. L. HALBERT, C. E. HUNTING, AND A. ZUCKER
Oak Ridge National Laboratory,* Oak Ridge, Tennessee

(Received October 5, 1959)

The differential cross section for the elastic scattering of nitrogen from thin carbon foils was measured from about 40 to about 140 deg in the center-of-mass system. The measurements were made at three energies: 27.3 Mev, 23.5 Mev, and 21.5 Mev, mean energy in the 1-Mev thick targets. The angular resolution was about 1 deg. Scattered nitrogen and recoil carbon atoms were counted in coincidence. Positions of the two counters, as prescribed by the kinematics of elastic scattering, served to discriminate against inelastic events and transfer reactions. The differential cross sections at all three energies exhibit marked structure especially beyond 90 deg. An optical model scattering calculation using a Saxon potential with $V=45$ Mev, $W=6$ Mev, and $a=0.65$ fermi was performed. The results of the calculation exhibit fair agreement with the data. The results of the experiment are also compared with the predictions of a sharp cutoff model for elastic scattering and show no agreement with the theory. Analyzing the data in terms of a diffraction model the positions of the well-defined minima yield an interaction distance R such that $r_0=1.18\pm0.02$ in the relation $R=r_0(A_1^{1/3}+A_2^{1/3})$.

INTRODUCTION

THE elastic scattering of nuclei by nuclei is of intrinsic interest because it may yield information on the behavior of gross nuclear matter. The earliest such experiments dealt with nitrogen-nitrogen scattering.¹ More recently the scattering of carbon from gold; and nitrogen, oxygen, and neon from bismuth has been studied.² In these experiments the scattered particles were detected with nuclear emulsions and identified by their range, a technique which is suitable only if the elastic cross section is large compared with those inelastic scattering or transfer reactions which might be confused with elastic scattering.

The situation is somewhat better with scintillation detectors which have been used to study the elastic scattering of oxygen from gold, nickel, aluminum and carbon.³

Recently a more powerful technique was employed at this laboratory in which the scattered and the recoil particle are detected in coincidence.⁴ The angles of both detectors and the pulse-height information from each are used to identify an event as elastic scattering, and to differentiate it from other reactions. This method allows measurement of differential elastic cross sections as small as several tenths of a millibarn/sr in the presence of large counting rates from other reactions. The coincidence technique, used first for elastic scattering of N^{14} by Be^9 , is here applied to another target element-carbon. Carbon was chosen because it can be readily prepared in thin self-supporting foils and its low-lying excited states are well separated from the ground state. Deviations from Rutherford scattering

were expected since the beam energy available exceeds the Coulomb barrier. In the present measurement, nitrogen-14 at 27.3, 23.5, and 21.5 Mev (mean laboratory energy in the target) was scattered from carbon foils and the differential cross section measured from about 40 to about 140 deg.⁵

EXPERIMENTAL PROCEDURE

The experimental procedure employed in this experiment was essentially identical with the one described in I. Two scintillation counters in coincidence were used inside a 24-in. diam scattering chamber, Fig. 1. A small aperture ($\frac{1}{4}$ deg half angle in the labora-

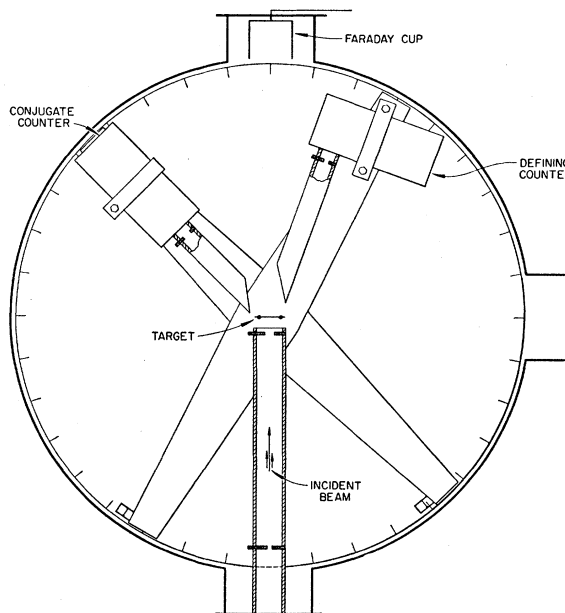


FIG. 1. Schematic drawing of the scattering chamber.

* Operated for the U. S. Atomic Energy Commission by Union Carbide Corporation.

¹ H. L. Reynolds and A. Zucker, Phys. Rev. **102**, 1378 (1956).

² E. Goldberg and H. L. Reynolds, Phys. Rev. **112**, 1981 (1959); Bull. Am. Phys. Soc. **4**, 253 (1959).

³ J. A. McIntyre, S. D. Baker, and T. L. Watts, Phys. Rev. **116**, 1212 (1959).

⁴ M. L. Halbert and A. Zucker, Phys. Rev. **115**, 1635 (1959). (Hereinafter this paper is referred to as I.)

⁵ All angles are in the center-of-mass system unless otherwise noted.

tory system) on the defining counter determined the solid angle. The aperture of the conjugate counter was always large enough to count all recoil particles from elastic events detected in the defining counter. Frequent experimental checks were made as outlined in I to verify that no coincidences were being lost. These checks included variation of conjugate-counter position, aperture, and threshold setting for the coincidence gating circuit.

Both counters were 0.005-in. CsI(Tl) on Lucite light pipes mounted on DuMont-6291 photomultiplier tubes. Linear amplifiers were used for pulse amplification. The pulses from the defining counter were analyzed with a 20-channel pulse-height analyzer, gated by the coincident pulses from the conjugate counter. The resolving time of the coincidence circuit was about 2.8 μ sec.

Reference I gives a detailed account of the design of this type of experiment, and we will not dwell on it here. The carbon experiments were considerably cleaner than the beryllium experiment because (1) the counting rate from oxygen impurity in the carbon targets was never more than a few percent of the carbon counting rate, (2) the inelastic events are well separated in angle and pulse height, (3) the transfer reactions are all endoergic and are also well separated from elastic events, and (4) counting rates from carbon were generally higher. Multiple scattering and the low energy of the coincident particles at some angles prevented us from measuring the cross section at angles smaller than 40 deg and larger than 144 deg.

From 40 deg to about 102 deg the defining counter was used to count nitrogens while the conjugate counter accepted recoil carbons. From 92 deg to the largest angles measured, carbons were counted in the defining counter and nitrogens in the conjugate counter for the reasons outlined in I. The ten-degree region between 92 and 102 deg provides an overlap which essentially checks the beam direction with respect to the defining counter position. At small angles and again at large ones the target was tilted toward the conjugate counter to reduce the energy loss in the target and decrease the effect of multiple scattering on the low-energy particles.

Mild steel magnetic shields were affixed to the counters and placed along the beam path to minimize the effect of the fringing field of the cyclotron on the paths of the particles. An antiscattering aperture was placed just below the target and a $\frac{1}{8}$ -in. diameter beam collimating aperture was near the entrance of the beam pipe. At full energy the angular divergence of the incident beam was at most 0.1 deg (lab). For reduced energy runs nickel or aluminum absorbers were placed on the beam collimator. The antiscattering aperture then limited the beam on the target to an angular divergence of about 1 deg (lab). All apertures were circular. Taking into account the angular acceptance

of the defining counter, the finite size of the beam spot on the target, multiple scattering, and angular divergence of the incident beam, the center-of-mass angular resolution is estimated to be about ± 1 deg for the full-energy data and about ± 2 deg for the two lower energy measurements.

Carbon targets were made by diluting a commercial alcohol suspension of colloidal graphite⁶ with ethyl alcohol until a fairly thin mixture was obtained. This was poured out on a clean glass plate and allowed to dry. The carbon film was carefully floated off in water and mounted on a thin plastic frame. Targets obtained in this way were between 150 and 200 μ g/cm² thick.

It was found that the counting rate from a given target gradually increased over a period of weeks. Presumably, carbon from the pump oil was being deposited on the target. To prevent this from affecting the results frequent runs were made at 60 deg. All data were normalized to these 60-deg runs. The absolute cross section at this angle was then measured in short runs using several foils which were weighed before and after bombardment.

The beam energy was lowered from 27.3 Mev mean energy in the target to 23.5 Mev by placing a 0.989 mg/cm² Ni absorber on the beam collimator. Upon substitution of a 1.269 mg/cm² Al foil, the mean energy was found to be 21.5 Mev. Each of these energies was measured by placing a hydrogen-filled chamber at the forward port of the scattering chamber, and measuring the range in emulsion of protons scattered at zero degrees. The energy loss in one target was determined by a fourth run in which the target was inserted in the beam. We thus had two methods for estimating the energy loss of the nitrogen ions in the carbon target. One was the direct measurement. Another method was to calculate the energy loss from the measured target thickness. The stopping power of carbon for nitrogen ions was calculated from the known stopping power of nickel and by using the relative stopping powers for carbon and nickel for protons of the same velocity as the nitrogen ions.⁷ The two estimates differed by about 8%, well within what one expects from either the accuracy of the measurement or the reliability of the calculation. Several targets were used in the course of the experiment. Care was taken to select only those targets whose thickness did not differ by more than 20% from the 1-Mev thick target which was used for the energy loss determination.

The targets contained C¹² and C¹³ in their normal isotopic fractions, 98.9% and 1.1%, respectively. The counter angles were always set according to the kinematics for N¹⁴-C¹² scattering. At the largest angles studied C¹³ scattering would have been completely rejected by the coincidence scheme, but at the smallest

⁶ "Dag" dispersion Number 154, obtained from Acheson Colloids Company, Port Huron, Michigan.

⁷ W. H. Webb, H. L. Reynolds, and A. Zucker, Phys. Rev. **102**, 749 (1956).

angles the counting rate probably included all elastic C^{13} events. All calculations were made on the basis of a C^{12} target. Unless the C^{13} cross section is more than an order of magnitude larger than the C^{12} cross section, the error introduced by assuming a pure C^{12} target is always smaller than the standard deviations quoted in the table of results.

Finally, because of our energy discrimination and angular resolution, we believe that no inelastic or transfer events from carbon, or scattering from impurities were confused with elastic scattering.

RESULTS

The results of this experiment are given graphically in Fig. 2. In addition we have tabulated the numerical values of the elastic scattering cross section and its ratio to the Coulomb cross section in Table I. The errors listed in the table are standard deviations of the relative cross sections. These include contributions from the following sources of error: (1) counting statistics, the major source of error at angles larger than 120 deg, (2) random errors in beam current measurement and integration, contributing about $\pm 2\%$ at all angles, (3) other sources such as uncertainties in background subtraction principally of importance at the largest angles. The error in setting the defining-counter angle is ± 0.1 deg (lab) corresponding to about ± 0.2 deg c.m.

In addition to the relative errors listed in Table I, there are systematic errors which do not change the shape of the angular distribution, but do affect the

absolute value of the cross section. These errors arise from uncertainties in (1) in the target thickness, purity, uniformity and angle; (2) the solid angle subtended by the defining counter; (3) the average charge of nitrogen ions emerging from the target; and (4) the beam-integrator calibration. All percent errors given below are estimated standard deviations.

The target thickness was determined by weighing the carbon foils and measuring their area. These measurements were subject to an error estimated to be $\pm 8\%$.

The uniformity of the targets is more difficult to evaluate. No measurable difference in the counting rate was found when various portions of a foil were used; data from four different targets gave the same results when normalized to the same target weight. The effect of nonuniformity is thus probably small compared to the 8% error in the thickness measurements themselves. The uncertainty in measuring the target angle produced an error smaller than 2% in the cross section.

The solid angle subtended by the defining aperture, computed from its diameter and its distance from the target, could have been in error by about 4%. The average charge was calculated from the equilibrium charge distribution for nitrogen in plastic foils.⁸ It also might have been in error by several percent. The absolute calibration of the beam integrator was uncertain by a similar amount. Fortunately these three uncertainties may be eliminated by measuring the counting rate for some process with a known cross section from a target of accurately known thickness. In effect one substitutes one error, that in the thickness of this secondary target, for the three uncertainties given above.

The process chosen for the absolute calibration was elastic scattering of nitrogen from a thin nickel foil. The available nitrogen energy is well below the Coulomb barrier for nickel, and the scattering cross section can therefore be calculated. It was found that over the entire range of defining counter settings used in the nickel scattering the cross section exhibits the expected $\csc^4(\theta/2)$ shape, thus providing a check on the measured laboratory angles. The N-C absolute differential cross section calculated from the measured solid angle, the estimated average charge of the beam, and the integrator calibration agreed with the cross section based on the nickel calibration to within 2%.

The uncertainty in the nickel thickness measurement was $\pm 3\%$. The root-mean-square error from all systematic factors was thus about 9%, due mostly to the uncertainty in the carbon target thickness.

At certain angles, notably around 100 deg and 135 deg, regions where the structure is most pronounced, some lack of reproducibility of the data was noted. This was investigated very extensively, and it was

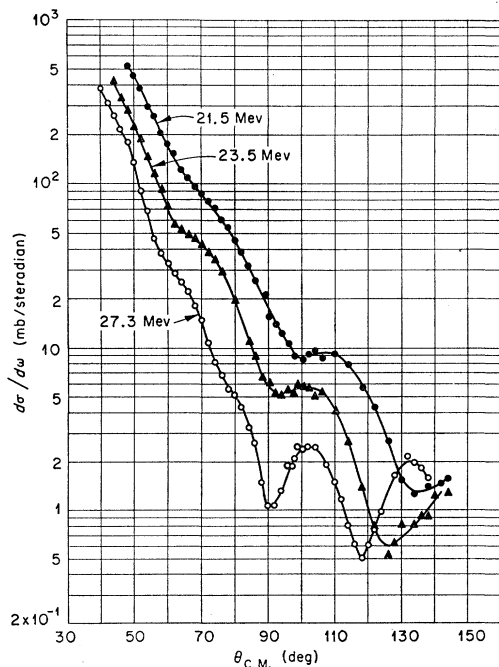


FIG. 2. The differential cross section of $N^{14}-C^{12}$ elastic scattering at 27.3 Mev, 23.5 Mev, and 21.5 Mev as a function of the nitrogen c.m. angle. Mean energies in the target are shown.

⁸ H. L. Reynolds, L. D. Wyly, and A. Zucker, Phys. Rev. **98**, 474 (1955).

TABLE I. Differential cross section for N^{14} - C^{12} elastic scattering and its ratio to Coulomb scattering.

Nitrogen c.m. angle (degrees)	27.3 Mev			23.5 Mev			21.5 Mev		
	$d\sigma/d\omega_{c.m.}$ (mb/sr)	Standard deviation ^a (percent)	$d\sigma/d\sigma_{Coul}$	$d\sigma/d\omega_{c.m.}$ (mb/sr)	Standard deviation ^a (percent)	$d\sigma/d\sigma_{Coul}$	$d\sigma/d\omega_{c.m.}$ (mb/sr)	Standard deviation ^a (percent)	$d\sigma/d\sigma_{Coul}$
40	382	5	0.363
42	309	5	0.354
44	262	5	0.358	411	5	0.416
46	214	5	0.346	330	5	0.396
48	179	5	0.341	282	5	0.397	520	5	0.613
50	134	5	0.298	221	5	0.363	452	5	0.621
52	89.9	5	0.231	185	5	0.351	385	5	0.613
54	68.6	5	0.202	147	5	0.320	296	5	0.541
56	45.8	5	0.155	113	5	0.283	258	5	0.540
58	37.9	5	0.145	92.2	5	0.262	205	5	0.488
60	33.1	5	0.144	72.7	5	0.234	176	5	0.473
62	28.3	5	0.139	57.1	5	0.207	153	5	0.465
64	25.5	5	0.140	53.2	5	0.216	122	5	0.414
66	22.1	5	0.135	48.6	5	0.220	109	5	0.413
68	18.2	5	0.123	47.1	5	0.237	97.0	5	0.409
70	14.9	5	0.112	43.1	5	0.240	84.6	5	0.395
72	10.8	5	0.0898	38.1	5	0.234	79.7	5	0.410
74	8.10	5	0.0738	34.4	5	0.232	71.1	5	0.402
76	6.86	5	0.0689	28.8	5	0.213	60.4	5	0.374
78	5.62	5	0.0612	54.7	5	0.370
80	5.16	5	0.0611	19.6	5	0.172	45.5	5	0.334
82	4.37	5	0.0562	38.9	5	0.310
84	3.30	5	0.0459	10.9	5	0.113	32.3	5	0.279
86	2.60	5	0.0391	8.89	5	0.0989	26.2	5	0.242
88	1.50	8	0.0242	6.61	5	0.0791
89	21.6	5	0.225
90	1.07	8	0.0185	6.07	5	0.0780	15.7	5	0.169
92	1.08	8	0.0200	5.31	10	0.0731	14.1	10	0.163
93.8	1.34	8	0.0265	5.18	10	0.0757
94	1.34	8	0.0266	12.7	10	0.156
96	1.89	8	0.0401	5.63	10	0.0884	10.8	10	0.142
97.1	1.82	8	0.0399	5.25	10	0.0855
98	2.09	10	0.0471	6.01	10	0.100	8.87	10	0.124
98.8	2.49	10	0.0573
100.5	2.05	10	0.0501	5.89	10	0.107	8.52	10	0.129
102	2.47	10	0.0625	5.79	10	0.109	9.20	10	0.145
104	2.48	10	0.0664	5.09	10	0.101	9.61	10	0.160
106	5.41	10	0.113	8.63	10	0.151
107.4	1.94	10	0.0567
110	1.50	10	0.0470	4.17	10	0.0965	9.24	10	0.179
112	1.16	10	0.0381
114	0.810	10	0.0278	2.68	10	0.0682	7.85	10	0.167
116	0.615	10	0.0221
118	0.509	10	0.0191	1.39	10	0.0387	5.69	10	0.132
120	0.615	10	0.0240
122	0.763	10	0.0310	0.795	10	0.0239	4.36	10	0.110
124	0.982	10	0.0414
126	0.528	10	0.0171	2.68	10	0.0728
128	1.65	10	0.0746	0.637	10	0.0214
130	0.807	10	0.0280	1.53	10	0.0446
132	2.15	10	0.104
134	1.99	10	0.0991	0.811	10	0.0299	1.27	10	0.0392
136	1.82	10	0.0932	0.901	10	0.0343
138	1.59	10	0.0836	0.913	10	0.0357	1.40	10	0.0460
140	1.24	10	0.0496
142	1.46	10	0.0503
144	1.29	10	0.0541	1.57	10	0.0554

^a The standard deviation is for random errors only. For systematic errors see text.

shown not to be due to counting losses, inhomogeneities in the target, errors in measuring beam intensities or fluctuations in beam direction. About the only factor over which we had no control and which could result in nonreproducible data is variation of the beam energy. The energy dependence of the cross section is quite pronounced and varies considerably from angle to

angle as can be seen from Fig. 2. If we take as a typical value from our results a factor of 0.65 as the change in cross section per Mev energy change, then a fluctuation of 1% in beam energy would effect about a 20% change in the cross section.

The beam energy is measured by the proton recoil technique. The uncertainty in this measurement is

± 300 kev out of ~ 27.8 Mev, or approximately $\pm 1\%$. It was not practical either to monitor the energy to 1% or to keep it constant within that amount. Instead all cyclotron parameters such as dee voltage, frequency, and deflector voltage were carefully monitored and kept as constant as cyclotron operation would allow. The best system to compensate for this effect as well as for the accretion of carbon on the target proved to be measuring cross sections at various angles alternately with the cross section at some fixed angle. We chose 60 deg for the fixed angle. A change in energy, then, would change the counting rate at 60 deg as well as at the angle investigated. This scheme worked especially well where the cross section is smooth. The points shown in Fig. 2 are averages of experimental data taken as ratios to 60 deg. At those angles where a change in energy produced a significant shift in the oscillatory pattern, the fluctuations could not be entirely eliminated by taking ratios to 60 deg. The remaining fluctuations are included in the standard deviations listed in Table I. Normalizing 60 deg runs at all three energies were taken on the same day, so that the relative cross sections are probably accurate to $\pm 3\%$.

The direction of the incident beam was determined in two ways: first, by burning a spot on a piece of tape placed over the defining collimator and, second, by measuring the cross section on both sides of the incident beam. This was done in the region between 92 and 102 deg. First the defining counter detected nitrogens and subsequently it detected carbons. At all three energies the sharp minima in the cross section occurred at the same angles with both modes of counting. We conclude, therefore, that the beam direction was constant and known to an angle at least equal to the angular resolution of the defining counter. The errors in the cross section produced by errors in angle setting are not significant in this experiment.

DISCUSSION

The field of nucleus-nucleus collisions is a relatively new one and no body of theory has been developed for it yet. Recently, however, much has been done to explain nucleon-nucleus scattering, particularly since the advent of the optical model of the nucleus.⁹ This model, first developed for neutron and proton scattering, has been adapted with satisfactory results to the scattering of deuterons and α -particles from various nuclei. It seemed, therefore, worth while to examine the possibilities this model offers for nucleus-nucleus scattering even though the physical relevance of the model is not apparent at this time.

This investigation is being made by R. H. Bassel, M. A. Melkanoff, and R. M. Drisko with the aid of IBM 704 and 709 computers. Preliminary results only

⁹ For recent references to papers on this subject see *Proceedings of the International Conference on the Nuclear Optical Model*, edited by A. E. S. Green, C. E. Porter, and D. S. Saxon (Florida State University, Tallahassee, 1959).

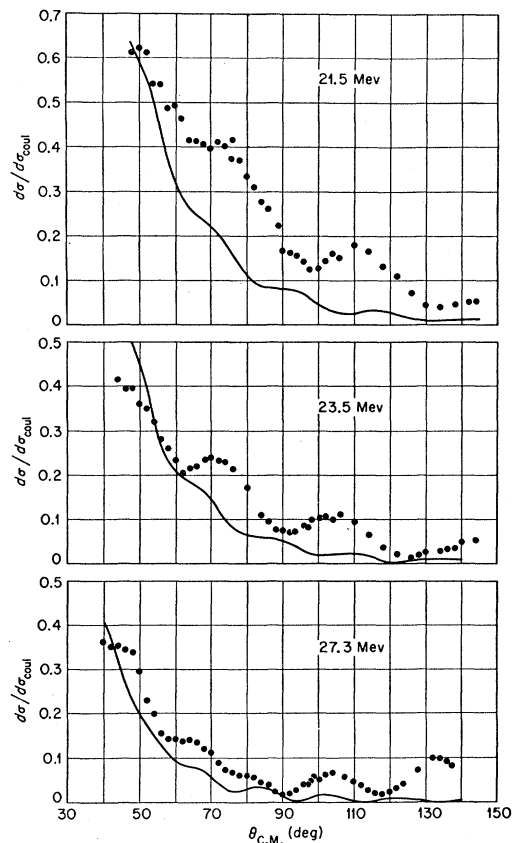


Fig. 3. Comparison of the data (shown as dots) with the results of some preliminary optical model scattering calculations (smooth lines). The optical model used a Saxon potential with the following parameters $V=45$ Mev, $W=6$ Mev, $a=0.65$ fermi, $r_0=1.32$ fermis. Comparisons at three energies are shown with the ratio of the elastic to Coulomb cross section plotted vs the nitrogen c.m. angle. The same optical parameters were used at the three energies.

are available; they produce fair fits with the data. Figure 3 shows the best fits so far obtained with a Saxon potential. The parameters which produce the best fits, $V=45$ Mev, $W=6$ Mev, $r_0=1.32$ fermis, and $a=0.65$ fermi are very much like optical model parameters deduced from nucleon-nucleus scattering. To be sure, the fits are not very good, but it must be borne in mind that they are the results of a very preliminary and incomplete search for parameters.

The maximum at 132 deg for the 27.3-Mev data seems to be especially difficult to fit. It may be that this is due to transfer-elastic events such as a deuteron transfer from the nitrogen to the carbon or a neutron exchange transfer, neither of which can be distinguished from elastic scattering.

The following argument for the applicability of the optical model calculations to N-C scattering was suggested by Breit.¹⁰ For close collisions the model constants are such that the wave disappears very

¹⁰ G. Breit (private communication).

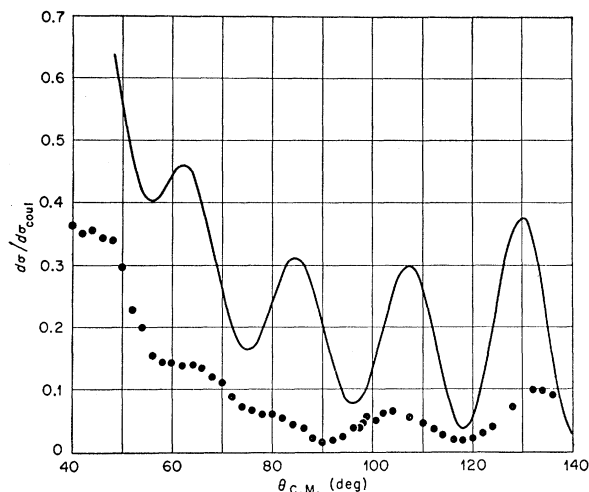


FIG. 4. Comparison of the 27.3-Mev data (shown as dots) with a sharp cutoff calculation (smooth curve) using $l_{\text{cutoff}}=7$. The ratio of the elastic to Coulomb cross section is plotted vs the nitrogen c.m. angle.

rapidly as the two particles interpenetrate. Therefore even though the model has no plausibility for strong interpenetration this particular fault of it should not be detrimental because the condition for inapplicability is not concerned with the most frequent events. In the N+C scattering the distance within which the probability of penetration is decreased to $1/2.718$ on account of the effect of W is $\sim 0.51 \times 10^{-13}$ cm. In this estimate it was assumed that $E - V_{\text{total}} = 0$. Now $V_{\text{total}} = V + V_{\text{Coul}}$ and for $r_0 = 1.32$ f the distance for contact is 6.20 f which gives $V_{\text{Coul}} = 9.71$ Mev. For $E_{\text{lab}} = 23.5$ Mev, i.e. $E_{\text{c.m.}} = 10.85$ Mev, there is available in the center-of-mass system at $r = 6.20$ f only 1.14 Mev kinetic energy. Unless the real part of the optical model potential sets in suddenly at contact, which is improbable $|E - V_{\text{total}}|$ is small compared with W and the absorption should be strong, as estimated. The attractive real potential of the optical model does not have a really strong influence until it becomes large. Thus if $|E - V_{\text{total}}| = W$ the decay length caused by absorption is increased only by about 25% in comparison with $E - V_{\text{total}} = 0$. The success of the optical model in giving approximate fits is therefore an indication of its qualitative correctness for the larger distances but says nothing regarding the interaction at small distances.

The sharp cutoff model for elastic scattering was developed by Blair¹¹ for cases where semiclassical approximations are expected to hold. It has produced good fits with elastic scattering experiments of nitrogen on nitrogen¹ and carbon on gold.² The Blair model has failed, however, to reproduce the data for N-Be scattering, I.

The differential cross section in this model is given by

$$\frac{d\sigma}{d\omega} = \left| \frac{-\eta}{2k \sin^2(\theta/2)} \exp[-i\eta \ln \sin^2(\theta/2)] e^{2i\delta_0} - \frac{1}{2ik} \sum_{l=0}^7 (2l+1) e^{2i\delta_l} P_l(\cos\theta) \right|^2.$$

The cutoff l value of 7 was calculated on the basis of the semiclassical relation

$$l(l+1) = (2\mu R^2/\hbar^2)(E - E_B),$$

where μ is the reduced mass, E the center-of-mass energy, E_B the Coulomb barrier, and $R = 1.5 (A_1^{1/3} + A_2^{1/3})$. The results of this calculation (carried out on an IBM 650) are compared with experimental results in Fig. 4. To point up the structure we compare $\sigma/\sigma_{\text{Coul}}$ rather than the cross sections themselves. The fit is not good. Some of the predicted positions of maxima and minima are reproduced by the data, but this may be fortuitous. Calculations with cutoff l values of 5, 6, 8, 9, yield equally unsatisfactory results and fail to reproduce the positions of the extrema. Calculations at the two lower energies fit the data no better. However, an improved fit is obtained if one uses larger cutoff l values than the ones obtained from the semiclassical relation above.

The sharp cutoff model is valid if $\eta = Z_1 Z_2 e^2/\hbar v$ is much larger than unity. At the energies investigated in this experiment the values of η are 4.8, 5.2, and 5.4. Also, it has been observed that in α -particle scattering¹² the model breaks down when $\sigma/\sigma_{\text{Coul}} < 1/\eta$. On this basis a good fit with the 27.3-Mev data would not be expected since $\sigma/\sigma_{\text{Coul}}$ is always smaller than $1/\eta$. For fairly large portions of the experimental results at the lower energies $\sigma/\sigma_{\text{Coul}} > 1/\eta$; nevertheless the agreement between the predictions of this theory and the measured cross sections is poor.

In α -particle scattering from light elements and nucleon scattering from heavy elements angular distributions similar to ours have been observed. These are sometimes interpreted as diffraction patterns. If one uses the Born approximation for scattering from a square well the positions of the extrema of the diffraction patterns can be approximated by those of the function $j_1(qR) = j_1[2kR \sin(\theta/2)]$, where j_1 is the spherical Bessel function, q the momentum transfer, k the wave number, and R the interaction radius. After the first few oscillations of the Bessel function this is equivalent to the statement that $R = (\pi/2k) \times \Delta \sin(\theta/2)$ where $\Delta \sin(\theta/2)$ is the interval between successive minima. Calculating $r_0 = R/(A_1^{1/3} + A_2^{1/3})$ in this way from the two most pronounced minima at each energy (between 90 and 135 deg), we obtain a value of $r_0 = 1.18 \pm 0.02$ fermis. The error here is just the standard deviation of the three values of r_0 . This is somewhat smaller than $r_0 = 1.32$ fermis employed in

¹¹ J. S. Blair, Phys. Rev. **95**, 1218 (1954).

¹² H. E. Wegner, R. M. Eisberg, and G. Igo, Phys. Rev. **99**, 825 (1955).

the optical model fitting, and considerably smaller than the value of $r_0 \sim 1.5$ fermis which is obtained from reaction cross sections.

ACKNOWLEDGMENTS

The authors are indebted to R. H. Bassel and M. A. Melkanoff for making the results of their

preliminary optical model calculations available before publication. They are also grateful to H. L. Reynolds and E. Goldberg for carrying out the Blair-model calculation. Our thanks go to A. W. Riikola and H. L. Dickerson for their operation of the cyclotron and to G. A. Palmer for his valuable assistance in taking data.

PHYSICAL REVIEW

VOLUME 117, NUMBER 6

MARCH 15, 1960

Single Particle Motion in a Deformed, Nonlocal Potential Well*

R. H. LEMMER†

Department of Physics, Florida State University, Tallahassee, Florida

(Received October 2, 1959)

The effects of the nonlocal character of the average nucleon-nucleus interaction on single particle motion in a strongly deformed field are examined by using a simple phenomenological description of the nonlocal interaction and introducing an effective mass approximation for a finite nuclear system.

The eigenvalues and eigenfunctions of the anisotropic harmonic oscillator potential are used as a starting point for a perturbative treatment of the nonlocal interaction, and the resulting energy level scheme is given as a function of the nuclear deformation. A conventional spin-orbit interaction has also been included in these calculations.

1. INTRODUCTION

IT is well known that the collective rotational and vibrational excitations observed in nuclei throughout most of the periodic table find a ready interpretation in terms of the Bohr-Mottelson collective model which in general embodies a complicated interweaving of single particle motion and collective motion of the nucleus as a whole.^{1,2} However, this unified description of nuclear motion simplifies considerably in the two limiting cases when the nucleus is almost spherical or has a strongly deformed equilibrium shape. Because of the close relation between the nuclear equilibrium shape and nucleon configuration, nuclei assume a near spherical equilibrium shape in the vicinity of closed shells and the collective excitations are predominantly of a vibrational character about the spherical shape. On the other hand, nuclei lying in regions between closed shells³ have a strongly deformed equilibrium shape as evidenced by the large quadrupole moments

The main effects of the nonlocal interaction appear as an increase in the level spacing of the unperturbed oscillator states combined with an additional interaction energy which can be interpreted as an effective angular momentum dependence of the average potential field.

Calculations of nuclear equilibrium deformations based on the computed level schemes are presented. It is found that the preponderance of prolate nuclear shapes found empirically can be accounted for quite well by the nonlocal model and results essentially from the favoring of high angular momentum substates that are introduced by the nonlocal interaction.

and pure rotational spectra observed for such nuclei.⁴ For large equilibrium deformations of this type one finds that the nuclear motion separates into collective and intrinsic single particle modes which are approximately independent of each other.⁵ The wave function of the nucleus can then be expressed as the product

$$\Psi = \Phi_{\text{coll}} \chi, \quad (1)$$

apart from some symmetrization terms.² Here Φ_{coll} describes the collective rotational motion of the nucleus and zero-point vibrations about the nonspherical equilibrium shape; χ denotes the intrinsic wave function for single particle motion in the average deformed field of the nucleus, which we will denote by $V(\mathbf{r})$ and which can be regarded as static if the period of rotation of the nucleus is much longer than a single particle period in the average field.⁵

The present discussion is confined to this latter region where the nuclear motion is adequately described by Eq. (1). In particular, we examine how the velocity dependence of the average nuclear field affects the intrinsic motion of the individual nucleons.

According to Eq. (1) the main features of nuclear rotational states are independent of the details of the intrinsic motion of the nucleons themselves. However,

* This work was partially supported by the U. S. Atomic Energy Commission.

† Present address: Physics Department, Massachusetts Institute of Technology, Cambridge, Massachusetts.

¹ A. Bohr and B. R. Mottelson, *Kgl. Danske Videnskab. Selskab, Mat.-fys. Medd.* **27**, No. 14 (1953).

² S. A. Moskowsky, *Handbuch der Physik* (Springer-Verlag, Berlin, 1957), Vol. XXXIX (a comprehensive recent review).

³ Large deformations are known to occur in nuclei with $155 < A < 185$ and $A > 225$. Nuclei around $A \sim 25$ also appear to exhibit rotational spectra, [G. Rakavy, *Nuclear Phys.* **4**, 375 (1957)].

⁴ The experimental data is summarized by K. Alder, A. Bohr, T. Huus, B. Mottelson, and A. Winther, *Rev. Modern Phys.* **28**, 432 (1956).

⁵ This is the strong-coupling approximation of A. Bohr.